

Electrons in Non-Homogeneous Magnetic Fields*

F. Peeters[†] and A. Matulis[‡]

Departement Natuurkunde, Universiteit Antwerpen (UIA)
Universiteitsplein 1, B-2610 Antwerpen, Belgium

Received July 12, 1993

The successful growth of a thin film ferromagnetic material on top of a semiconductor has opened a new and exciting field in solid state physics. Lithographic patterning of the ferromagnetic film will allow one to construct nonhomogeneous magnetic fields on a length scale of nanometers which may interact with a two-dimensional electron gas underneath the film. The electrons moving from a zero magnetic field region towards a nonzero magnetic field region will feel this region as a barrier. New systems are proposed consisting of magnetic tunneling barriers: 1) magnetic quantum wires, 2) double tunneling barriers, 3) magnetic dots, 4) magnetic superlattices, etc. The form of the equivalent potential that corresponds to a magnetic barrier depends on the wavevector of the incident electron. This renders the transmission through such structures an inherently *two-dimensional* process since the tunneling probability depends not only on the electron's energy but also on the direction of its wavevector. Pronounced resonances are obtained for the tunneling probability and the conductance of a resonant tunneling device consisting of such magnetic barriers. Such systems can be used as an electron wavevector filter. The energy spectrum (bound and scattered states) for these systems is obtained and the nature of the states is discussed.

I. Introduction

The behavior of electrons in *macroscopically* homogeneous magnetic fields has been used extensively to obtain experimental information on properties of charge carriers^[1] like e.g. their density and the Fermi surface (through the Shubnikov de Haas (SdH) effect), and their mass (e.g. using cyclotron resonance). Scattering of electrons on magnetic impurities form the other limit in which electrons feel locally (on an angstrom scale) strong magnetic fields (i.e. *microscopically* inhomogeneous) which may act as scattering centers in e.g. diluted semimagnetic materials^[2].

Between these limits lie inhomogeneous magnetic fields on the *nanometer* scale. They have recently been realized with the creation of magnetic dots^[3], integration of ferromagnetic materials with semiconductors^[4-6] where patterning of such films was

recently demonstrated experimentally^[7]. This new technology will add a new functional dimension to the present semiconductor technology and will open new avenues for new physics and possible applications like, switches based on the Lorentz force and non-volatile memories based on the Hall voltage generated by a local magnetic field. A different route to create inhomogeneous magnetic fields is through the integration of superconducting materials with semiconductors. This was realized experimentally using type II superconductors which was deposited on a Si-MOS^[8] or a GaAs/AlGaAs-heterojunction^[9,10]. Magnetic flux lines penetrate the two-dimensional electron gas (2DEG) acting as nanoscale scattering centers for the electrons^[11-13], offering the possibility to study weak localization^[10] and the dynamics of vortices^[14]. Using lithographic techniques these superconducting films can be patterned into any desired form. The ge-

*Invited talk.

[†]Email: peeters@nats.uia.ac.be

[‡]Permanent address: Semiconductor Physics Institute, Gostauto 11, 2600 Vilnius, Lithuania.

ometry of the patterning determines the geometry of the inhomogeneous magnetic field.

In general the shape anisotropy of the magnetic film (or the stripes) will force the magnetization in the plane of the film. Other mechanisms can be active which can lead to a magnetization vector perpendicular to the film, which is the situation we are mostly interested in. Out-of-plane magnetization has been realized in ultrathin layers of Fe on Ag^[15] or Cu^[16], compounds such as MnAlGa^[17], Co/Ni^[18] multilayers, and ultrathin MnGa films^[5] and the metastable τ -MnAl phase^[4] which can be grown epitaxially on GaAs/AlAs heterostructures using MBE.

The creation of superlattices by an inhomogeneous magnetic field was proposed theoretically in Refs. [19] and [20]. Vilms and Éntin^[21] presented a theoretical analysis of the energy spectrum of 2D electrons near domain walls and in a system of parallel magnetic strips. Transport of a 2DEG in the presence of a perpendicular magnetic field modulated weakly and periodically along one direction was studied in Ref. [22] and recently tried unsuccessfully experimentally by Yagi and Iye^[23]. The generalization to 2D magnetic field modulation is given in Ref. [24]. Recently Van Roy *et al.*^[25] studied the geometric factors controlling the magnitude of the demagnetizing field of ferromagnetic thin films with perpendicular magnetization. Different geometries were studied and they found that a grating-type structure with periodicity of a few 100nm to 1 μ m would give the maximum magnetic field strength in the underlying semiconductor heterostructure. Müller^[26] considered a different system in which a 2DEG strip is placed in a perpendicular magnetic field which increases linearly along one direction. He showed that this system has a remarkable time-reversal symmetry. The present authors^[27] studied different systems consisting of magnetic barriers and considered also tunneling through double magnetic barriers^[28]. A quasi-analytic solution to a model barrier system was found in Ref. [29].

In the present paper we will consider different configurations of nonuniform magnetic fields in which the nonuniformity is only along one direction and has a typical length scale of the order of nanometers. The electron spectrum of a 2DEG in simple magnetic structures like, magnetic step (Sect. III), magnetic barrier (Sect. IV) and magnetic well (Sect. V) is considered and discussed. The similarities and differences between similar potential problems is pointed out. We consider electron tunneling through structures of magnetic barriers and in particular resonant tunneling. In contrast with tunneling through electric barriers, the tunneling probability depends not only on the electron's energy but also on the direction of its wavevector. This renders the tunneling an *inherently two-dimensional* process. Furthermore we found that the magnetic barriers possess wavevector filtering properties.

II. Nonhomogeneous magnetic field profiles

As shown in Fig. 1 a magnetic barrier can be created by the deposition, on top of a heterostructure, of a ferromagnetic stripe with magnetization (a) perpendicular and (b) parallel to the 2DEG, (c) of a conducting stripe with a current driven through it, and (d) of a type I superconducting plate interrupted by a stripe. In all cases the 2DEG is situated at a distance z_0 below the stripe whose thickness and height are d and h , respectively.

For the case of magnetic stripes we consider the following Maxwell equations

$$\begin{aligned} \text{div } \vec{B} &= -4\pi \text{div } \vec{M} = 4\pi \rho_M(\vec{r}), \\ \vec{B} &= -\text{grad } \Phi_M, \end{aligned} \quad (1)$$

which can be integrated and results into

$$\Phi_M(\vec{r}) = \int d^3r' \frac{\rho_M(\vec{r}')}{|\vec{r} - \vec{r}'|}. \quad (2)$$

For illustrative purposes we consider perpendicular magnetization (Fig. 1(a)) in which the width of the magnetic strip d is very small such that we can replace it by a dipole line with magnetic charge density:

$\rho_M(\vec{r}) = -M_0\delta(x)\frac{d}{dz}\delta(z)$. Integrating (2) results in the magnetic potential

$$\Phi_M(\vec{r}) = \frac{2M_0z}{x^2 + z^2}. \quad (3)$$

which leads to the magnetic field distribution

$$B(x) = 2M_0 \frac{z_0^2 - x^2}{(z_0^2 + x^2)^2}, \quad (4)$$

and the vector potential

$$A(x) = 2M_0 \frac{x}{z_0^2 + x^2}. \quad (5)$$

If we have stripes of width d instead of wires we have to integrate Eq.(2) numerically in the region $-d/2 \leq x' \leq d/2$. It turns out that in the limit $z_0, h \ll d$ the magnetic field distribution takes the simple form (h is the height of the magnetic strip)

$$B(x, z_0) = B_0 (K(x + d/2, z_0) - K(x - d/2, z_0)) \quad (6)$$

with $B_0 = Mh/d$ and $K(x, z) = 2xd/(x^2 + z^2)$ which is depicted in Fig. 2(a) for three values of z_0 . Similarly for parallel magnetization we found $K(x, z) = -zd/(x^2 + z^2)$ and which is depicted in Fig. 2(b) for three values of z_0 .

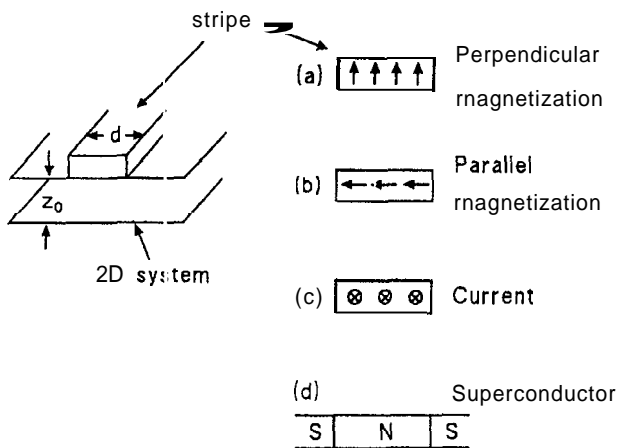


Figure 1: Sectional view of several systems for producing non-homogeneous magnetic field profiles in the plane of the 2D electron gas.

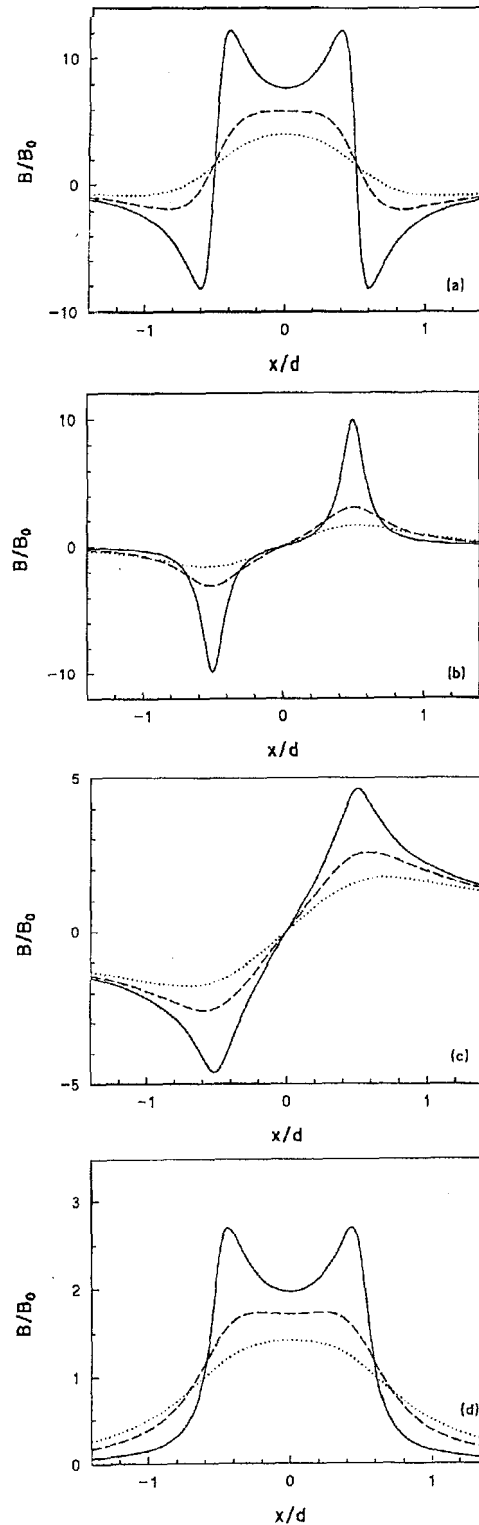


Figure 2: Magnetic field under the stripe corresponding to the four different configurations as given in Fig.1. The magnetic field is given at different distances from the magnetic stripe: $z_0 = 0.1$ (solid curve), $z_0 = 0.3$ (dashed curve), and $z_0 = 0.5$ (dotted curve).

For a wire with a current I going through it (Fig. 1(c)) the magnetic field is determined by the Maxwell equation: $rot \vec{B} = 4\pi \vec{j}/c$ which results in the angular

magnetic field component $B_\phi = 2I/cr$ at a radial distance r from the wire. In the plane of the 2DEG a distance z_0 from the wire this leads to the magnetic field profile

$$B(x) = B_z(x, z_0) = B_0 \frac{x}{z_0^2 + x^2}, \quad (7)$$

with $B_0 = 2I/c$ which is depicted in Fig. 2(c). The vector potential is obtained by integrating the equation $\vec{B} = \text{rot}\vec{A}$ which gives

$$A(x) = A_y(x, z_0) = \frac{1}{2} B_0 \ln \left(\frac{z_0^2 + x^2}{z_0^2 + R^2} \right), \quad (8)$$

where R is some distance away from the wire where the opposite current is flowing. For a strip of finite width d such that $z_0, h \ll d$ we can cast the result into the form of Eq.(6) with $K(x, z) = \ln[(x^2 + z^2)/d^2]$. This magnetic field profile is shown in Fig. 2(c).

For a superconducting stripe in a magnetic field we have to solve the Maxwell equations in the superconductor: $\vec{j} = -(ne^2/mc)\vec{A}$, and $\nabla^2 \vec{H} = (1/L_0^2)\vec{H}$, where $L_0^2 = mc^2/4\pi ne^2$ and we made use of $\text{rot}\vec{H} = -(4\pi ne^2/mc^2)\vec{A}$. Outside the superconductor we have the equation: $\nabla^2 \Phi_M = 0$, with the boundary condition on the superconductor $B_n = -\partial\Phi_M/\partial n = 0$. This 2D potential problem can be solved by the conformal mapping $x + ir = \sin(\pi w)$ where we introduce the complex potential $W = \Phi_M + i\Psi$. The solution of the problem is $W = iw$ and the magnetic potential is given by $\Phi_M = \text{Re}W = -\text{Im}(\arcsin(x + iz))$ which results into the magnetic field $B = B_0 \text{Re}(1/\sqrt{1 - (x + iz)^2})$ as shown in Fig. 1(d).

The magnetic field produced by the stripes, in units of B_0 , is shown in Fig. 2 for three different depths: $z_0 = 0.1$ (solid curve), $z_0 = 0.3$ (dashed curve) and $z_0 = 0.5$ (dotted curve). The smaller z_0 , i.e., the closer the 2DEG is to the stripes, the sharper the magnetic barrier structure. With increasing z_0 the magnetic field profile becomes gradually smoother. Concurrently with the magnetic field profile one expects a scalar (electric) potential, which can be short circuited by putting a non-magnetic metallic film^[23] between the 2DEG and

the patterned layer and which therefore will be neglected.

III. Motion in nonhomogeneous magnetic fields

We consider a 2DEG moving in the (x, y) plane with a magnetic field \mathbf{B} along the z -direction. In the single-particle approximation such a system is described by the hamiltonian

$$H = \frac{1}{2m} (\mathbf{p} + \frac{e}{c} \mathbf{A})^2 \quad (9)$$

We take the vector potential in the Landau gauge $\mathbf{A} = (0, A, 0)$ and the magnetic field is uniform along the y -direction but modulated along the x -direction, and thus

$$B_z = B(x) = \frac{d}{dx} A(x), \quad (10)$$

where we have the magnetic field profiles of previous section in mind.

Let us introduce the following characteristic parameters: i) the frequency $\omega_c = eB_0/mc$ with B_0 some typical magnetic field, and ii) the length $\ell_B = \sqrt{\hbar c/eB_0}$. For GaAs and an estimated $B_0 = .1\text{T}$ we have $\ell_B = 813\text{\AA}$, $\hbar\omega_c = .17\text{meV}$, and $\ell_B\omega_c = 1.4m/sec$. From now on we will express all quantities in dimensionless units: 1) the magnetic field $B(x) \rightarrow B_0 B(x)$, 2) the vector potential $A(x) \rightarrow B_0 \ell_B A(x)$, 3) the time $t \rightarrow t/\omega_c$, 4) the coordinate $\mathbf{r} \rightarrow \ell_B \mathbf{r}$, 5) the velocity $\mathbf{v} \rightarrow \ell_B \omega_c \mathbf{v}$, and 6) the energy $E \rightarrow \hbar\omega_c E$.

In these dimensionless units the two-dimensional (2D) Schrödinger equation becomes

$$\left\{ \frac{\partial^2}{\partial x^2} + \left(\frac{\partial}{\partial y} + iA(x) \right)^2 + 2E \right\} \Psi(x, y) = 0. \quad (11)$$

Because of the special form of the gauge the system is translational invariant along the y -direction and as a consequence we can choose the following form for the wavefunction

$$\Psi(x, y) = e^{-iqy} \psi(x) \quad (12)$$

where $-q = k_y$ is the wavevector of the electron in the y -direction which is a conserved quantity. This does

not imply that v_y is conserved. The wavefunction $\psi(x)$ actually satisfies the following 1D Schrödinger equation

$$\left\{ \frac{d^2}{dx^2} - (A(x) - q)^2 + 2E \right\} \psi(x) = 0 \quad (13)$$

where the function

$$V(x) = \frac{1}{2}(A(x) - q)^2 \quad (14)$$

can be interpreted as a q -dependent electrical potential. Note that in the case of one-dimensional (1D) magnetic field modulation studied in the present paper there is an analogy between the magnetic field and the potential given by the following relation

$$B(x) = \frac{1}{\sqrt{2V(x)}} \frac{dV(x)}{dx}. \quad (15)$$

A jump in the magnetic field will result in a discontinuity in the derivative of the potential $V(x)$.

IV. Magnetic step

First, let us consider the most simple shape for a nonhomogeneous magnetic field: the magnetic step. In this situation the magnetic field fills the half space $x > 0$ which is described by $B(x) = \theta(x)$ with the corresponding vector potential $A(x) = x\theta(x)$, where $\theta(x) = 1(x \geq 0), 0(x < 0)$ is the step-function. There are two different cases which we have to consider.

Case 1 ($q > 0$). The potential $V(x) = \frac{1}{2}(x\theta(x) - q)^2$ has the form of an asymmetric quantum well which deepens with increasing q . It is well-known^[30] that such a well can have a bound state if the well is sufficiently deep. Thus, we have to consider separately: a) $E < q^2/2$ where bound eigenstates are expected to appear in the region $x \sim q$, and b) $E > q^2/2$ which corresponds to scattered states, describing the electron reflection by the magnetic step. The appearance of bound states makes this system essentially different from the usual potential step problem where only scattered states exist.

For Case 2 ($q < 0$) the equivalent potential is a constant $V(x) = q^2/2$ for $x < 0$, and a barrier $V(x) = \frac{1}{2}(x\theta(x) + |q|)^2$ in the region $x > 0$ which is

unbounded for $x \rightarrow \infty$. In this case there are only scattered states which corresponds to electron reflection by the magnetic barrier.

For $x > 0$ the Schrodinger equation takes the form

$$\left\{ \frac{d^2}{dz^2} - \frac{z^2}{4} + p + \frac{1}{2} \right\} \psi(z) = 0. \quad (16)$$

with $z = \sqrt{2}(x - q)$ and $p = E - 0.5$. The solutions of it are the Weber functions^[31] $D_p(z)$ which have the following asymptotic behaviour: $D_p(z)|_{z \rightarrow +\infty} \rightarrow 0$. In the region $x > 0$ the wavefunction becomes $\psi(x) \sim D_{E-0.5}(\sqrt{2}(x - q))$, up to a normalization constant, while for $x < 0$ there is no magnetic field and the wavefunction is proportional to $\psi(x) \sim \exp(x\sqrt{q^2 - 2E})$ when $E < q^2/2$. Matching the wavefunctions and its first derivative at $x = 0$ we obtain the following equation

$$\sqrt{q^2 - 2E} = \frac{d}{dx} \ln D_{E-0.5}(\sqrt{2}(x - q)) \Big|_{x=0}. \quad (17)$$

whose solutions lead to the electron eigenvalues $E = E_n(q)$ with the corresponding wavefunction $\psi_{nq}(x)$.

Once we know the eigenvalues and the corresponding wavefunction we can obtain the other characteristics of the bound states. The average electron velocity of the bound state along the magnetic step (y -direction)

$$-v_n(q) \equiv \int_{-\infty}^{\infty} dx x \psi_{nq}^2(x) (q - A(x)) = \frac{d}{dq} E_n(q), \quad (18)$$

where the minus sign results from the definition $q = -k_y$. The mean electron position along the z -axis $X_n(q)$ has the simple form

$$\begin{aligned} X_n(q) &= \int_{-\infty}^{\infty} dx x \psi_{nq}^2(x) \\ &= q + \left(1 + \frac{1}{2q\sqrt{q^2 - 2E_n(q)}} \right) v_n(q). \end{aligned} \quad (19)$$

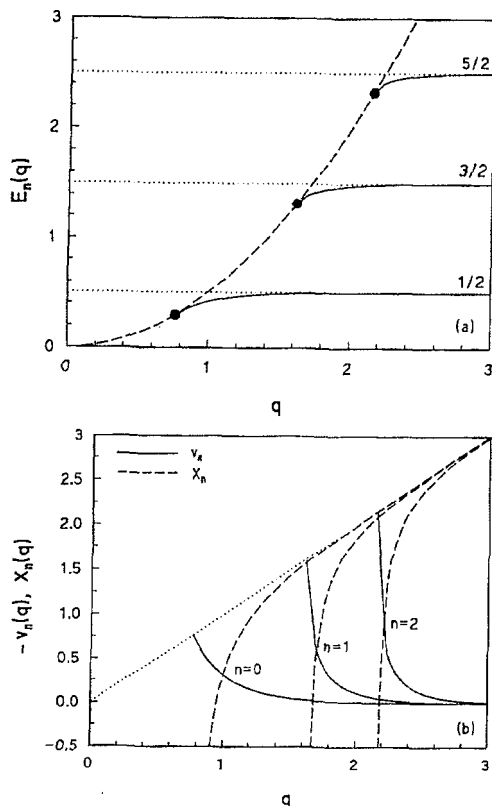


Figure 3: a) the energy spectrum for the bound states (solid curves), and b) the corresponding average velocity along the magnetic step $v_n(q)$ (solid curves) and the electron average position $X_n(q)$ along the x -axis (dashed curve) for the magnetic step case.

The numerical results of the solution of Eq. (17) are depicted in Fig. 3(a) by the solid curves, for the lowest three eigenvalues. These curves start at a certain q -value (denoted by the solid dot in Fig. 3), which is a function of n . The corresponding results for the average electron velocity $v_n(q)$ (solid curves) and mean electron position $X_n(q)$ (dashed curves) are shown in Fig. 3(b). Notice that the eigenvalues asymptotically, i.e. $q \rightarrow \infty$, reach the values $(n + 1/2)$ for Landau levels in a homogeneous magnetic field as it should be. In this asymptotic limit the mean electron position approaches $X_n(q) \sim q$ and the average electron velocity tends to zero. In this limit the electron is situated far from the magnetic step and is not influenced by the $x < 0$ region. With decreasing q the electron wavefunction starts to feel the magnetic step: 1) its energy decreases, because part of the wavefunction will be situated in a region with zero magnetic field where the electron will have a smaller kinetic energy, 2) its aver-

age position is less than q , because the wavefunction is sucked into the $x < 0$ region, and 3) its velocity increases and the electron runs along the step. From Figs. 3(a) and 3(b) we notice that the width of the transition region, i.e. the q -region where $E_n < (n + 1/2)$, is narrower with increasing n . The above properties of these bound states forces us to make the analogy with edge states^[32]. Nevertheless there are a number of differences: 1) the available q -space for edge states increases with increasing Landau level number n which is opposite to the behavior of the present bound states, 2) the direction of the velocity is opposite as compared to those of the usual edge states; and 3) the magnitude of the velocity satisfies $|v_n(q)| \leq q$ which is different from edge states which do not have an upper bound on their velocity.

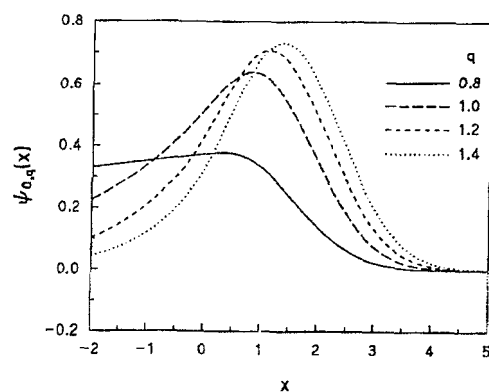


Figure 4: The electron wavefunction for the lowest bound state for different values of the electron momentum in the y -direction (q) in the case of a magnetic step.

From Fig. 3 we notice that there exist critical values q_n^* such that for $q < q_n^*$ no bound states are found. These points are indicated by the dots on Fig. 3(a) and are situated on the free electron spectrum curve $E = q^2/2$ (dashed curve in Fig. 3(a)). For the plotted curves we found the critical values: $q_0^* = 0.768$, $q_1^* = 1.623$, $q_2^* = 2.155$ at which the eigenenergy curve $E_n(q)$ is tangent to the $E = q^2/2$ curve. At these points the electron velocity equals the free electron value: $-v_n = q$, and $X_n(q) \rightarrow -\infty$. The electron wavefunction $\psi_{n,q}(x)$ is shown in Fig. 4 for the $n = 0$ case and different values of the wavevector q . This figure

nically illustrates the increasing leakage of the wavefunction into the $x < 0$ region with decreasing q -value and the concomitant increasing asymmetry of the wavefunction.

Notice that in the present magnetic step case the transmission coefficient is always zero. Independent of the strength of the magnetic field and the magnitude of the electron energy an electron, impeding on the magnetic barrier will always be reflected, which is a consequence of the Lorentz force acting on the electron. In this respect this system is different from the textbook potential step problem in which the reflection coefficient becomes different from zero when the electron energy is larger than the potential barrier height.

V. Magnetic barrier

The magnetic step can be used as a building block, from which more complicated structures can be built. As a first example we consider the magnetic barrier in which the magnetic field is different from zero in a strip of width d . In this case the magnetic field has the following form in dimensionless units: $B(x) = \theta(d^2/4 - x^2)$, and we choose the vector potential as follows: $A(x) = -d/2$ ($x < -d/2$), x ($|x| \leq d/2$), $d/2$ ($x > d/2$). The analogous potential $V(x)$ of (14) depends on the value of the wavevector q : when $|q| < d/2$ the potential consists of an asymmetric well of finite height, and when $|q| > d/2$ it is a gradual step. The problem is symmetric under the substitution $q \rightarrow -q$ (and $x \rightarrow -x$) and consequently we may limit ourselves to the case $q \geq 0$.

There are three different energy regions important to us: 1) $0 \leq E \leq (d/2 - q)^2/2$ where bound eigenstates can exist, 2) $(d/2 - q)^2/2 < E \leq (d/2 + q)^2/2$ which is the reflection region, and 3) $(d/2 + q)^2/2 < E$ where the electron is transmitted through the magnetic barrier.

First let us concentrate on the situation in which we have bounded electron states. In this case the electron wavefunction in the barrier region, i.e. $|x| < d/2$, is a

linear combination of Weber functions

$$\psi(x) = aD_{E-0.5}(\sqrt{2}(x-q)) + bD_{E-0.5}(\sqrt{2}(q-x)) \quad (20)$$

which we must match (and its first derivative) to the free electron wavefunctions at the points $x = \pm d/2$. This matching results into the equation

$$F^+(-q+d/2)F^-(q+d/2) - G^+(q-d/2)G^-(-q-d/2) = 0 \quad (21)$$

where

$$F^\pm(z) = \sqrt{(q \pm d/2)^2/2 - E} D_{E-0.5}(\sqrt{2}z) + D'_{E-0.5}(\sqrt{2}z) \quad (22)$$

and

$$G^\pm(z) = \sqrt{(q \pm d/2)^2/2 - E} D_{E-0.5}(\sqrt{2}z) - D'_{E-0.5}(\sqrt{2}z). \quad (23)$$

Eq. (21) was solved numerically. The results for a wide magnetic barrier ($d = 5$) are shown in Fig. 5 by the solid curves which end at the solid dots. The latter are situated on the $E = (q - d/2)^2/2$ curve (dashed curve). Notice that the spectrum resembles the one of the magnetic step case (see Fig. 3(a)) with the distinction that the latter has an infinite number of branches while the one for a magnetic barrier has a finite number of bound states for each q . For $d = 5$ there are only three branches in the energy spectrum. The number of energy branches decreases with decreasing barrier width d . Irrespective of the value of d there is always *at least one* discrete energy value for $q = 0$. This is a consequence of the fact that for $q = 0$ the potential $V(x)$ is one-dimensional and symmetric. Such a potential is known to have at least one discrete eigenvalue^[30] irrespective of the size of the potential well. The value of the lowest branch in the spectrum is plotted in Fig. 6 for $q = 0$ as function of the barrier width d . Notice that when $d < 1$ (i.e. when the magnetic barrier width is less than the magnetic length l_B) the eigenvalue approaches $E_0(q = 0) \approx (d/2)^2/2$ which is shown by the long-dashed curve in Fig. 6. Although the electron is bound to the barrier, in the case of small d -values the electron wavefunction is situated mainly outside the barrier and

consequently its energy approaches the height of the potential well $V(d/2)$. The width in q -space (Δq) of the lowest energy branch is also given in Fig. 6. It is seen that this width decreases rapidly to zero when $d < 1$ and in the opposite case (when $d \rightarrow \infty$) it asymptotically reaches the line $\Delta q/2 = d/2 - q_0^*$ (short-dashed line). Where $q_0^* = 0.768$ is the value as obtained from the magnetic step spectrum. Another distinction as compared to the magnetic barrier spectrum (see Fig. 3(a)), is that the energy eigenvalues are smaller in magnitude than those in the magnetic step case.

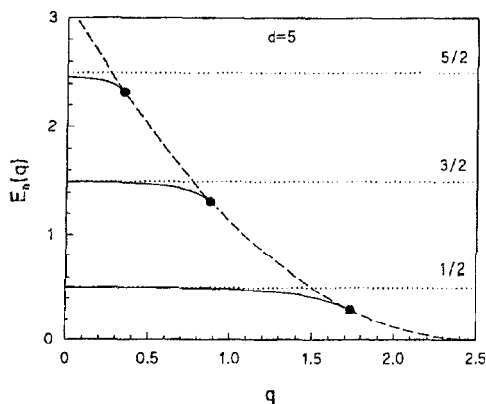


Figure 5: The energy spectrum for the bound states (solid curves) in a magnetic barrier of width $d = 5$. Dashed curve $E = (d/2 - q)^2/2$ indicates the free electron spectrum.

For the unbounded states we have calculated the transmission coefficient which now depends not only on the electron energy but also on the electron wavevector q in the y -direction. In the present case tunneling is a two-dimensional process in which the total electron wavevector and the electron energy is conserved but the direction of the wavevector is altered. A contour plot of the transmission coefficient $T(q, E)$ versus initial electron velocity components (v_x, v_y) is shown in Fig. 7 for a magnetic barrier of width $d = 5$. The quantum transition coefficient is zero above the line $v_y = (v_x^2 - d^2)/2d$ which is the result one would obtain from classical mechanics and which defines a semi-infinite transmission window. Below this line we have classically $T = 1$, but quantum mechanically $T(q, E)$ gradually increases with increasing electron energy. For rather thick barriers (as in the case of $d = 5$) there is

some additional structure at low energy which is enlarged in the inset of Fig. 7. There is an additional peak around $(v_x, v_y) = (0.3, -2.5)$ which is a consequence of the presence of a virtual energy level above the quantum well $V_q(x)$.

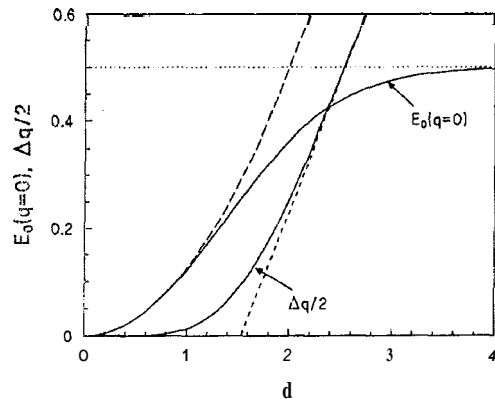


Figure 6: The lowest eigenvalue of the bound state in a magnetic barrier as function of the barrier width for $q = 0$ and the width (Δq) of the lowest energy branch in q -space (solid curves). The long-dashed curve indicates the height of the potential $V_{q=0}(x = d/2) = d^2/8$ and the short-dashed line $\Delta q/2 = d/2 - q_0^*$ indicates the asymptotic value of that width defined from the magnetic step spectrum.

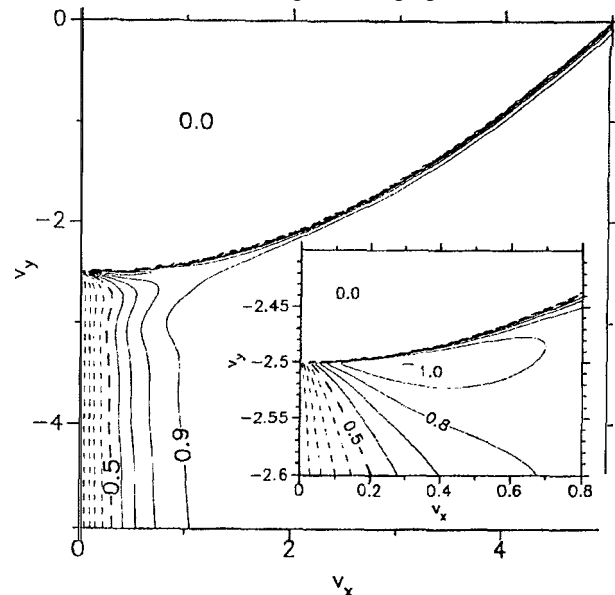


Figure 7: Contour plot of the transmission coefficient through a magnetic barrier of width $d = 5$ in the incident electron velocity (v_x, v_y) -space.

VI. Magnetic wire

The inverse situation of the previous problem is the magnetic well case which we will discuss now. Because of the essential 2D character of the electron motion in a magnetic field we should rather speak of a magnetic wire. In dimensionless units the magnetic field

is given by: $B(x) = 0$ ($|x| \leq d/2$), 1 ($|x| > d/2$), and the corresponding vector potential is: $A(x) = x - d/2$ ($x > d/2$), 0 ($|x| \leq d/2$), $x + d/2$ ($x < -d/2$). The value of the vector potential is now unbounded, i.e. $A(x)|_{x \rightarrow \pm\infty} \rightarrow \pm\infty$: and as a consequence the potential satisfies: $V(x)|_{x \rightarrow \pm\infty} \rightarrow \infty$ which implies that the electron motion is confined in the x -direction and *all the states are bound* at least in this direction.

The corresponding wavefunctions are constructed by matching the quasi-free electron wavefunction in the region $|x| < d/2$ with the Weber functions: $\psi(x) = D_{E-0.5}(\pm\sqrt{2}(x \mp d/2 - q))$, which are valid in the regions $|x| > d/2$. This matching of the wavefunction and its first derivative leads to the following algebraic equation for the eigenvalues

$$\left[\cos(kd)D_{E-0.5}(\sqrt{2}q) - \frac{\sqrt{2}}{k} \sin(kd)D'_{E-0.5}(\sqrt{2}q) \right] D'_{E-0.5}(-\sqrt{2}q) + \left[\cos(kd)D'_{E-0.5}(\sqrt{2}q) + \frac{k}{\sqrt{2}} \sin(kd)D_{E-0.5}(\sqrt{2}q) \right] D_{E-0.5}(-\sqrt{2}q) = 0, \quad (24)$$

where $k = \sqrt{2E - q^2}$ for $2E > q^2$ and $k = i\sqrt{q^2 - 2E}$ for $2E < q^2$ in which case the trigonometric functions should be replaced by their corresponding hyperbolic functions.

The results of the numerical solution of this equation are presented in Figs. 8(a) for a wide well (i.e. $d = 5$), and (b) for a narrow well (i.e. $d = 1$). In the wide well case (Fig. 8(a)) there are clearly two distinct regions which are separated by the free electron energy $E = q^2/2$ curve (dashed curve in Fig. 8(a)). For $E \ll q^2/2$ the energy spectrum consists of Landau levels. The electron is mainly located in the barrier where there exists a uniform magnetic field. For small q -values, i.e. $E \gg q^2/2$, the spectrum consists of bands with free electron-like motion in the y -direction. This is similar to the case of the well-known quantum wire with electrical potential barriers. When we decrease the width of the well the two regions are less distinct as is apparent in Fig. 8(b) for the case of $d = 1$. For $d = 1$ the well is narrower than the width of the electron wavefunction and consequently there is always an appreciable overlap of the wavefunction with the magnetic barrier region. Notice that the energy levels have

almost no dispersion. The different behavior between the two cases is also illustrated in Fig. 9 where the electron velocity is shown for the different states. Notice that the velocity exhibits a maximum near $E = q^2/2$ and it diminishes fast for $q \gg \sqrt{2E}$ which is the region where the electron is mainly located inside the magnetic barrier. Notice that for wide wells, i.e. see the $d = 5$ case, the velocity curve $v_n(q)$ can have several local maxima's which is a consequence of the repulsion of the different energy levels as seen in Fig. 8(a). In the case of the usual quantum wire constructed from walls consisting of potential barriers the electron velocity is $v_n = \hbar k_y = -q$ and is independent of the energy level index n and is a uniform increasing function of the electron wavevector. The behavior of $v_n(q)$ as depicted in Figs. 9 is also different from the one of edge states in which $v_n(q)$ is a uniform increasing function of q .

The density of states (DOS) for the two cases is depicted in Fig. 10. Notice that like for the quantum wire case the DOS exhibits singularities at the onset of each energy level. But there is a difference, the width in energy space of each level is finite and bounded by a singularity in the DOS. Suppose we have a system in

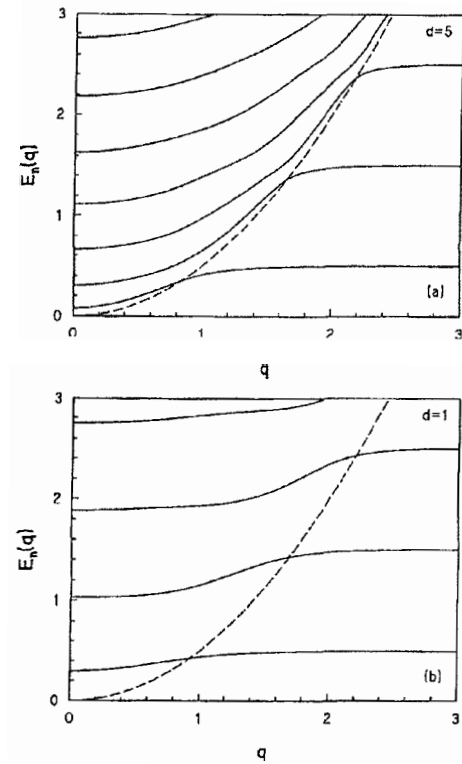


Figure 8: The energy spectrum of a magnetic well for two different values of the width: a) $d = 5$, and b) $d = 1$.

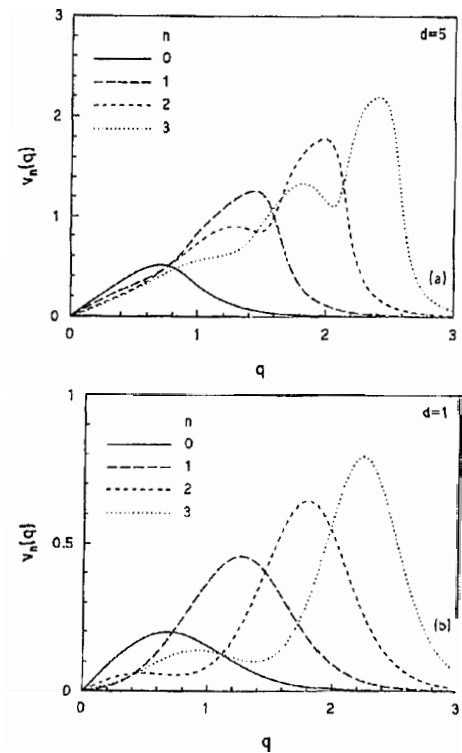


Figure 9: The electron average velocity corresponding to the energy spectrum of Fig. 6.

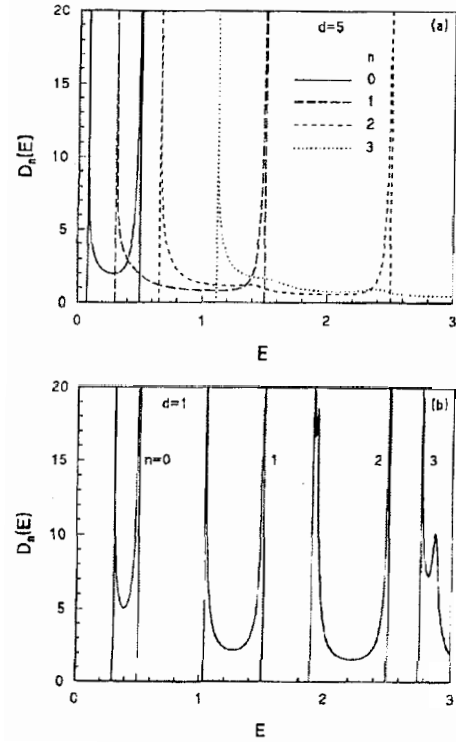


Figure 10: The density of states of the electron states in the magnetic wells corresponding to Fig. 6.

which we are able to increase the Fermi energy gradually. Starting from zero we first populate the quantum wire states, the electrons are mainly situated in the well region. Further increasing the Fermi energy we see that for $d = 5$ we first start to populate the next energy level which consists initially of states located inside the well. For $d = 1$ on the other hand we start to populate states which are situated in the magnetic barrier region and which are nothing else than 2D Landau states. Thus by changing the Fermi level we are able to have 1D states or 2D states at the Fermi level which will have considerable influence on the electrical properties of the system. The 1D states are quasi-free while the 2D states are localized on Landau orbits and can only move if scattering is involved.

VII. Resonant tunneling structures

In previous sections we have made a detailed study of the nature of the electron states in different magnetic barrier structures. In this section we will consider different tunneling structures where we will focus on the tunneling current going through it.

For simplicity we now consider electron tunneling through a magnetic barrier of constant height B_0 and width $d = x_+ - x_-$ surrounded by regions of zero magnetic field. The free electron wavefunction on the left side of the barrier ($z < x_-$) is $\psi_-(x) = Ae^{ik_-(x-x_-)} + Be^{-k_-(x-x_-)}$ and on the right side of it ($z > x_+$) $\psi_+(x) = e^{ik_+(x-x_+)}$, where $k_{\pm} = \sqrt{2[E - V(\pm\infty)]}$ is the x component of the electron wavevector on the corresponding side of the barrier. Under the barrier there are two solutions for $\psi(x)$ which can be written as a linear combination of the Weber function $D_p(x)$ and its derivative $D'_p(z)$. Next we construct the transition matrix

$$T(x, x_0) = \begin{pmatrix} u(x) & v(x) \\ u'(x) & v'(x) \end{pmatrix}, \quad (25)$$

where we defined the functions $u(x) = c\{D'_p(\sqrt{2q})D_0(z) + D'_p(-\sqrt{2q})D_0(-z)\}$ and $v(x) = c\{D_p(\sqrt{2q})D_0(z) - D_p(-\sqrt{2q})D_0(-z)\}$, with $p = E - 1/2$ and $z = \sqrt{2}(x - q)$, which satisfies the boundary conditions $u(x_0) = 1$, $u'(x_0) = 0$, $v(x_0) = 0$, and $v'(x_0) = 1$. Matching the wave function at the edges of the barrier, x_{\pm} , by means of the above matrix we obtain

$$A = T_{11}^{-1} + \frac{k_+}{k_-} T_{22}^{-1} + i \left(\frac{1}{k_-} T_{21}^{-1} - k_+ T_{12}^{-1} \right); \quad (26)$$

the electron transmission through the barrier $t(E, q)$ is given by

$$t(E, q) = \frac{k_+}{k_1 A|^2}, \quad (27)$$

where T^{-1} stands for the inverse of the matrix \mathbf{T} in $T(x_+, x_-)$. For complex structures involving several barriers of constant height, the total \mathbf{T} matrix is a product of the \mathbf{T} matrices that correspond to the separate barriers and the one describing the free electron propagation between the barriers. As for the electron current through such a structure! it can be calculated, in the ballistic regime, by introducing the conductance G as the electron flow averaged over half the Fermi surface^[33]

$$G = G_0 \int_{-\pi/2}^{\pi/2} t(E_F, \sqrt{2E_F} \sin \phi) \cos \phi d\phi, \quad (28)$$

where ϕ is the angle of incidence relative to the x direction. Further, $G_0 = e^2 m v_F \ell / \hbar^2$, where ℓ is the length

of the structure in the y direction and v_F the Fermi velocity.

To reveal the main qualitative features of tunneling through these barriers we restrict ourselves to: *i*) a single barrier which was already discussed in Sect. V, and *ii*) complex structures composed of rectangular magnetic barriers one example of which is shown in the inset of Fig. 11.

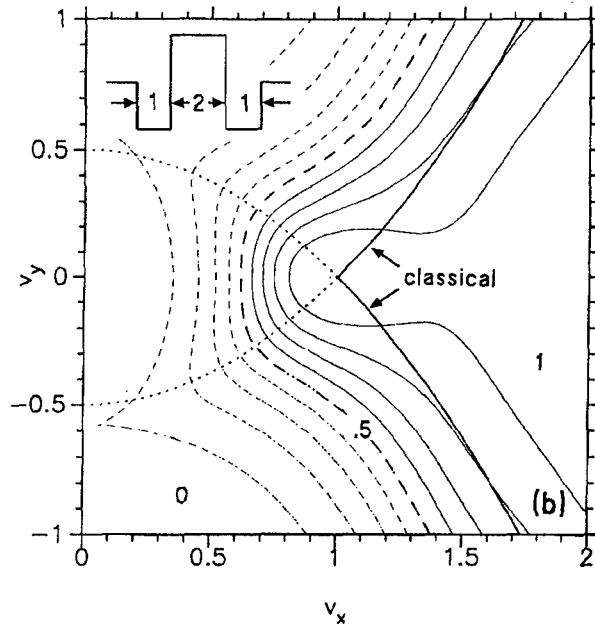


Figure 11: Contour plot of the electron transmission probability in the (v_x, v_y) plane for a more complex structure. The magnetic field profile of the corresponding magnetic barrier are shown in the inset of the figure.

The contour plot of the transmission through a complex structure, shown in the inset of Fig. 11, is presented in the figure. Notice that the quantum and the classical calculation give drastically different results.

This complex structure can be used as a building block to make a double barrier-like structure which is composed of two units identical to that of Fig. 11 with a zero field region, of length $L = 3$, between them. We show only the velocity contour plot in Fig. 12 and the corresponding classical result. Again we see sharp resonances, the wavevector filtering properties, and the strong dissimilarity between the quantum and classical results.

Having seen the transmission results, one may wonder to what extent their structure is reflected in measurable quantities which involve some kind of averaging. In Fig. 13 we show the conductance, as given by Eq. (28), for the previous tunneling structure shown in the inset of the figure, together with the corresponding classical result (dotted curves). Despite the averaging of $t(E, q)$ over half the Fermi surface, we have again strong resonant structure. This structure will become sharper if one can select the wavevectors that give the sharpest resonance in the transmission. In principle this can be achieved using quantum point contacts. As for the classical result, we see again that they are determined only by the first barrier in each structure.

Although our consideration of electron tunneling through the rectangular magnetic barrier structures gives only a qualitative picture, nevertheless these resonant tunneling spikes should be present in the more realistic cases with barriers of smooth shape, cf. Fig. 2. Indeed these spikes do not depend on the actual shape of the magnetic barrier but only on the presence of barriers in the potential $V(x)$.

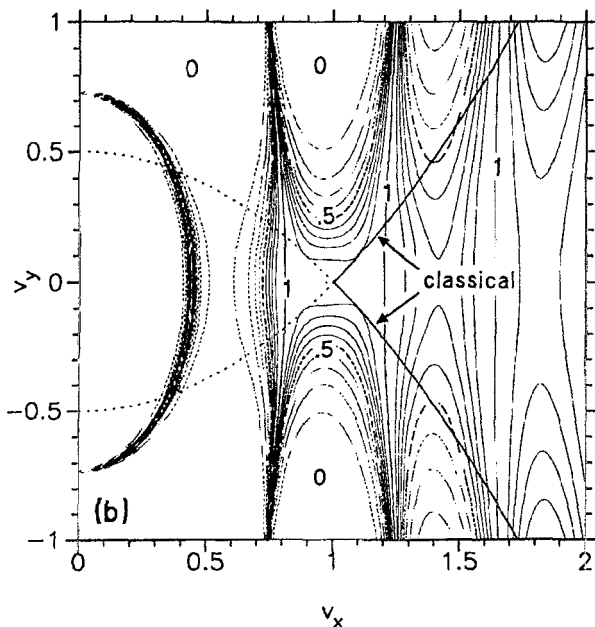


Figure 12: Contour plot of the electron transmission probability in the (v_x, v_y) plane for the resonant tunneling structure composed of the complex barrier structure of Fig. 11 in which the barriers are separated by the distance $L = 3$.

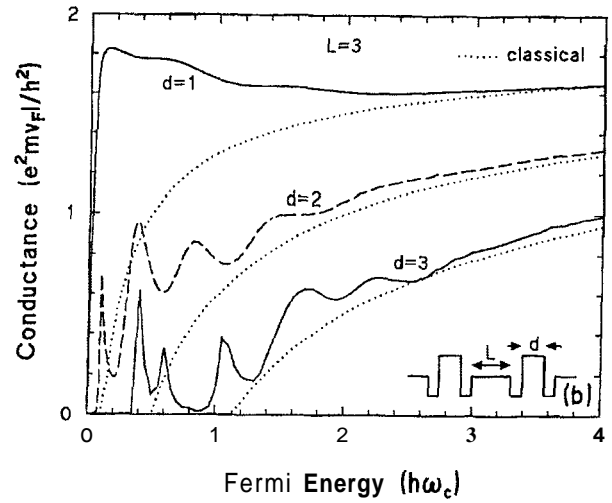


Figure 13: The conductance through the barrier structure shown in the inset for different values of the barrier parameters. The dotted curves show the conductance calculated classically.

VIII. Conclusion

The spectra of electrons moving in 2D and interacting with nonhomogeneous magnetic fields was calculated. Different structures of nonhomogeneous magnetic fields in one direction are considered. The similarities and differences between similar structures built from electrical potentials are pointed out. The motion in the present case is essentially 2D while in the electrical potential problems often a separation of variables is possible which reduces the problem to 1D. In the present case the problem can be mathematically cast into a 1D problem but the physics and the motion stays essentially 2D. In the magnetic case the potential $V(x)$ appearing in the mathematical 1D problem depends on the electron wavevector (q) which makes it inherently two dimensional even in the case of one-dimensional magnetic field modulations.

One of the interesting features of nonhomogeneous magnetic field structures is that a step in the magnetic field can bind electrons. The spectrum has bounded and unbounded (scattered) states. The wavefunction of the former are confined to the region with non-zero magnetic field. The discrete and continuum part of the spectrum overlap in an energy range. This is essentially different from potential steps which act always

repulsively. As a consequence magnetic barriers can exhibit bound states and tunneling through them turns out to be much richer: for example tunneling can occur through such bound states which may lead to quasi resonances in the transmission coefficient. Tunneling is essentially a 2D process where only transmission is possible in a semi-infinite window in velocity space. Such a magnetic barrier structure can be used as a filter for electron wavevectors. A combination of such magnetic barriers will result in more complicated structures, like for example resonant tunneling structures and superlattices.

We found that the quantum transmission through magnetic-barrier structures: i) depends not only on the energy but also on the direction of the wavevector, ii) possesses wavevector filtering properties, iii) shows well-pronounced resonances whereas the classical one does not, and iv) is drastically different from the classical transmission which is determined only by the sum of the barriers and is independent of the distance L between them.

We have shown that the physics of electron transport in nonhomogeneous magnetic fields is a rich subject. Furthermore one can think about creating magnetic dots, the theoretical analysis of which is in progress. Other possible systems are magnetic superlattices. In this case we may distinguish: 1) weak magnetic superlattices in which there is only a very weak modulation of the magnetic field. This problem was studied in Ref. [22] in which Weiss oscillations were predicted in the magneto-resistance which are a consequence of a commensurability between the period of the superlattice and the diameter of the cyclotron orbit, and 2) strong magnetic superlattices in which we may have: a) the situation of alternating magnetic wells and magnetic barriers such that the average magnetic field is zero. This system is now similar to the Kronig-Penney model, and b) the case with only magnetic barriers. Now the average magnetic field is non zero and as a consequence the electric potential $V(x)$, Eq.(14), is un-

bounded and all the states will be localized in the direction of the superlattice. The study of these problems is in progress.

Acknowledgments

This work is supported by the Belgian National Science Foundation (NFWO) and by the Interuniversity Microelectronics Center (IMEC, Leuven). One of us (AM) acknowledges the support of the EEC through the programme 'Cooperation in Science and Technology with Central and Eastern European Countries'. One of us (FMP) acknowledges fruitful discussions with P. Vasilopoulos.

References

1. D. Shoenberg, *Magnetic oscillations in metals*, (Cambridge University Press, Cambridge, 1984).
2. For a review see e.g. J. K. Furdyna, J. Appl. Phys. **64**, R29 (1988).
3. M. A. McCord and D. D. Awschalom, Appl. Phys. Lett. **57**, 2153 (1990).
4. T. Sands, J. P. Harbison, M. L. Leadbeater, S. J. Allen, Jr., G. W. Hull, R. Ramesh and V. G. Keramidas, Appl. Phys. Lett. **57**, 2609 (1990); M. L. Leadbeater, S. J. Allen, Jr., F. DeRosa, J. P. Harbison, T. Sands, R. Ramesh, L. T. Florez and V. G. Keramidas, J. Appl. Phys. **69**, 4689 (1991); T. Sands, J. P. Harbison, S. J. Allen, Jr., M. L. Leadbeater, T. L. Cheeks, M. J. S. P. Brasil, C. C. Chang, R. Ramesh, L. T. Florez, F. DeRosa and V. G. Keramidas, Mater. Res. Soc. **231**, 341 (1992).
5. M. Tanaka, J. P. Harbison, J. DeBoeck, T. Sands, B. Philips, T. L. Cheeks, and V. G. Keramidas, Appl. Phys. Lett. **62**, 1565 (1993).
6. K. M. Krishnan, Appl. Phys. Lett. **61**, 2365 (1992).
7. W. Van Roy, E. L. Carpi, M. Van Hove, A. Van Esch, R. Bogaerts, J. De Boeck, and G. Borghs, J. Magnetism and Magnetic Mater. **121**, 197 (1993).

8. J. H. R. u o and J. M. Klapwijk, in *Proceedings of the 19th Int. Conf. on the Phys. of Semicond.* (Warsaw, Poland, 1988). Edited by W. Zawadzki (Polish Academy of Sciences, Warsaw, 1989), p. 499.
9. A. K. Geim, Pis'ma Zh. Eksp. Teor. Fiz. **50**, 359 (1989) [JETP Lett. **50**, 389 (1990)]; A. K. Heym, S. V. Dubonos and A. V. Khaetskii, Pis'ma Zh. Eksp. Teor. Fiz. **51**, 107 (1990) [JETP Lett. **51**, 121 (1990)].
10. S. J. Bending, K. von Klitzing and K. Ploog, Phys. Rev. Lett. **65**, 1060 (1990).
11. J. Rammer and A. L. Shelankov, Phys. Rev. **B36**, 3135 (1987).
12. A. V. Khaetskii, J. Phys. **C3**, 5115 (1991).
13. L. Brey and H. A. Fertig, Phys. Rev. **B48** (1993).
14. G. H. Kruithof, P. C. van Son, and T. M. Klapwijk, Phys. Rev. Lett. **67**, 2725 (1991).
15. B. T. Jonker, K. H. Walker, E. Kisher, G. A. Prinz and C. Carbone, Phys. Rev. Lett. **57**, 142 (1966).
16. L. Liu, E. R. Moog and S. D. Bader, Phys. Rev. Lett. **60**, 2422 (1988).
17. R. C. Sherwood, E. A. Nesbitt, J. H. Wernick, D. D. Bacon, A. J. Kurtzig and R. Wolfe, J. Appl. Phys. **42**, 1704 (1971).
18. G. H. O. Daalderop, I. J. Kelly and F. J. A. den Broeder, Phys. Rev. Lett. **68**, 682 (1992).
19. B. A. Dubrovin and S. I. Novikov, Zh. Eksp. Teor. Fiz. **79**, 1006 (1980) [Sov. Phys. JETP **52**, 511 (1980)].
20. D. Yoshioka and Y. Iye, J. Phys. Soc. Japan **56**, 448 (1987).
21. P. P. Vil'ams and M. V. Éntin, Fiz. Tekh. Poluprovodn. **22**, 1905 (1988) [Sov. Phys. Semicond. **22**, 1209 (1988)].
22. P. Vasilopoulos and F.M. Peeters, Superlatt. and Microstr. **4**, 393 (1990); F.M. Peeters and P. Vasilopoulos, Phys. Rrv. **B47**, 1466 (1993).
23. R. Yagi and Y. Iye, J. Phys. Soc. Jpn. **62**, 1279 (1993).
24. X.-G. Wu and S. E. Ulloa, Phys. Rev. **B48** (1993).
25. W. Van Roy, J. De Boeck, and G. Borghs, Appl. Phys. Lett. **61**, 3056 (1992).
26. J. E. Müller, Phys. Rev. Lett. **68**, 385 (1992).
27. F. M. Peeters and A. Matulis, Phys. Rev. **B48**, 15166 (1993).
28. A. Matulis, F. M. Peeters and P. Vasilopoulos, in Proc. of the Int. Conf. EP2DS-10, (Newport, USA, 1993). Phys. Rev. Lett. **72**, (1994).
29. M. Calvo, Phys. Rev. **B48**, 2365 (1993).
30. *Quantum mechanics*, L.D. Landau and E. Lifshitz (Pergamon Press, Oxford, 1977), p.66.
31. *Handbooch of Mathematical Functions*, edited by M. Abramowitz and I. Stegun (Dover Publications, Inc., New York, 1972), p. 687.
32. Hajdu, in *Physics of the two-dimensional electron gas*, edited by J.T. Devreese and F.M. Peeters (Plenum, N.Y., 1987), p.27.
33. M. Büttiker, Phys. Rev. Lett. **59**, 1761 (1986).